PsbP-induced protein conformational changes around Cl^- ions in the water oxidizing center of photosystem II

J. KONDO and T. NOGUCHI+

Division of Material Science, Graduate School of Science, Nagoya University, Furo-cho, Chikusa-ku, Nagoya, 464-8602, Japan

+Corresponding author; tel.: +81-52-789-2881, fax: +81-52-789-2883, e-mail: tnoguchi@bio.phys.nagoya-u.ac.jp.

Abbreviations: DCMU – 3-(3,4-dichlorophenyl)-1,1-dimethylurea; FTIR – Fourier transform infrared; Mes – 2-(*N*-morpholino)ethanesulfonic acid; PMS – phenazine methosulfate; WOC – water-oxidizing center.

Acknowledgments: This study was supported by the Grants-in-Aid for Scientific Research from the Ministry of Education, Culture, Sports, Science and Technology (17H03662 to T.N.).

Abstract

PsbP is an extrinsic protein of photosystem II (PSII) having a function of Ca^{2+} and Cl^- retention in the water-oxidizing center (WOC). To understand the mechanism how PsbP regulates the Cl^- binding in WOC, we examined the effect of PsbP depletion on the protein structures around the Cl^- sites using Fourier transform infrared (FTIR) spectroscopy. Light-induced FTIR difference spectra upon the $S_1 \rightarrow S_2$ transition were obtained using Cl^--bound and NO_3^--substituted PSII membranes in the presence and absence of PsbP. A clear difference in the amide I band changes by PsbP depletion was observed between Cl^--bound and NO_3^--substituted PSII samples, indicating that PsbP binding perturbed the protein conformations around the Cl^- ion(s) in WOC. It is suggested that PsbP stabilizes the Cl^- binding by regulating the dissociation constant of Cl^- and/or an energy barrier of Cl^- dissociation through protein conformational changes around the Cl^- ion(s).

Additional key words: Mn_4CaO_5 cluster; oxygen evolution; photosynthesis.

Introduction

Photosystem II (PSII) is a multiprotein complex that has a function of oxygen evolution by water oxidation in oxygenic photosynthesis performed by plants and cyanobacteria. The catalytic site of water oxidation is the water-oxidizing center (WOC) that consists of the Mn_4CaO_5 cluster, two Cl^- ions, and surrounding amino acid residues (Umena *et al.* 2011, Suga *et al.* 2015). In the WOC, two water molecules are oxidized into one molecular oxygen and four protons by abstraction of four electrons using light energy (Messinger *et al*. 2012, Grundmeier and Dau 2012, Vinyard *et al*. 2013, Shen 2015). The electrons from water are transferred to the primary quinone electron acceptor Q_A and then to the secondary quinone acceptor Q_B, which becomes a quinol upon double reduction and is released into thylakoid membranes (Petrouleas and Crofts 2005). The thus abstracted electrons are finally used to reduce CO_2 to synthesize sugars. Reactions in WOC are performed by a cycle of five intermediates called S_i states (i = 0–4) (Joliot *et al*. 1969, Kok *et al*. 1970). The reaction starts from the dark-stable S_1 state, and it advances to the S_2 state upon one-electron oxidation. Likewise, S_2 advances to the S_3 state and then to the S_4 state, which is a transient intermediate and immediately relaxes to the S_0 state by releasing a molecular oxygen. The S_0 state is oxidized to the S_1 state to complete a reaction cycle.

Amino acid residues that ligate or directly interact with the Mn_4CaO_5 cluster and two Cl^- ions (designated Cl-1 and Cl-2) are all provided from the D1, D2 and CP43 subunits, which are membrane-spanning intrinsic proteins (Umena *et al*. 2011, Suga *et al*. 2015). However, some extrinsic proteins attached to the lumenal side of PSII are necessary for stabilizing the WOC structure and optimizing water oxidation activity

(Seidler, 1996, Enami *et al*. 2008, Ifuku, *et al*. 2008, 2011, Fagerlund and Eaton-Rye 2011, Bricker *et al*. 2012, 2013, Ifuku and Noguchi 2016, Roose *et al*. 2016). PsbO, PsbP, and PsbQ are the extrinsic proteins involved in PSII of higher plants, while cyanobacteria have PsbV and PsbU in addition to PsbO as major extrinsic proteins. The localizations of these extrinsic proteins in PSII complexes have been revealed by X-ray crystallography (Umena *et al*. 2011, Suga *et al*. 2015) or cryo-electron microscopy (Wei *et al*. 2016). Among the extrinsic proteins in higher plants, the role of PsbP has been extensively studied (reviewed in Ifuku 2008, 2011, Ifuku and Noguchi 2016, Bricker *et al*. 2013; Roose *et al*. 2016), and its major function was shown to be the retention of Ca^{2+} and Cl^{-} ions in WOC. To understand the mechanism of this PsbP function, the effect of PsbP binding on the structure of WOC has been investigated using light-induced Fourier transform infrared (FTIR) difference spectroscopy (Tomita *et al*. 2009, Ido *et al*. 2012, Kakiuchi *et al*. 2012, Nishimura *et al*. 2014, 2016). This spectroscopy is a powerful method to detect the structural changes of active sites upon reactions in photo-sensitive proteins, and has been extensively used to study the structure and reactions of WOC (Noguchi and Berthomieu 2005, Chu 2013, Debus 2015, Noguchi 2015). It was shown that PsbP depletion from spinach PSII induced protein conformational changes in WOC (Tomita *et al*. 2009). Similar conformational changes were also detected by depletion of some extrinsic proteins in PSII complexes from a red algae (Uno *et al*. 2013) and a cyanobacterium (Nagao *et al*. 2015). From these observations, it was proposed that PsbP in higher plants and some extrinsic proteins in other phyla play a role in retaining the protein conformations of WOC to regulate its reaction (Tomita *et al*. 2009, Nagao *et al*. 2015, Ifuku and Noguchi 2016). However, the

molecular mechanism how PsbP specifically regulates the binding properties of Ca^{2+} and Cl^- in WOC remains to be clarified.

In this study, we investigated the effect of PsbP on the protein structures of the Cl^- binding sites of WOC using light-induced FTIR difference spectroscopy. For this purpose, we examined the effect of replacement of Cl^- with NO_3^- on the PsbP-induced structural changes in WOC, which were detected by FTIR difference measurement upon the $S_1 \rightarrow S_2$ transition. It has been shown that NO_3^- substitution for Cl^- retains O_2 evolution activity but with a decreased efficiency in the $S_3 \rightarrow S_0$ transition (Sinclair 1984, Wincencjusz *et al*. 1999, Hasegawa *et al*. 2004, Suzuki *et al*. 2012). It is predicted that NO_3^- substitution induces perturbations in the protein moieties around Cl^- ions. The obtained results clearly showed that PsbP binding affects the protein conformations around the Cl^- ions, which should cause the alteration in the binding properties of the Cl^- ions in WOC.

Materials and methods

Oxygen-evolving PSII membranes of spinach were prepared as reported previously (Ono and Inoue 1986) and suspended in a pH 6.5 buffer (Cl^--buffer: 40 mM Mes-NaOH, 400 mM sucrose, 40 mM NaCl, 5 mM $Ca(OH)_2$, pH 6.5). For treatment of NO_3^-, the PSII membranes were suspended (0.5 mg Chl mL^{-1}) in a buffer involving 40 mM NO_3^- (NO_3^--buffer: 40 mM Mes-NaOH, 400 mM sucrose, 40 mM $NaNO_3$, 5 mM $Ca(OH)_2$, pH 6.5), and washed twice with the same buffer by centrifugation. A buffer involving $Na^{15}NO_3$ (Shoko Co. Ltd., 99.1 atom %) instead of natural abundance $NaNO_3$ ($Na^{14}NO_3$) was used for $^{15}NO_3^-$ treatment. For depletion of the PsbP and PsbQ proteins,

the PSII membranes were suspended (0.5 mg Chl mL^{-1}) in the Cl^--buffer additionally involving 2 M NaCl and incubated for 20 min on ice under dark (the PAGE image of the PsbP, Q-depleted PSII prepared by this treatment was presented in Fig. S1 of Tomita et al. 2009). The sample was then washed twice with the Cl^--buffer or three times with the NO_3^--buffer by centrifugation.

For $S_2Q_A^-/S_1Q_A$ FTIR measurements, 1 mL of the sample suspension (0.5 mg Chl mL^{-1}) in the Cl^-- or NO_3^-- buffer in the presence of 0.1 mM 3-(3,4-dichlorophenyl)-1,1-dimethylurea (DCMU) and 0.5 mM phenazine methosulfate (PMS) was centrifuged at 170,000 g for 35 min to obtain a pellet. In the case of Q_A^-/Q_A FTIR measurement, the last buffer for centrifugation additionally involved 10 mM NH_2OH, which depletes the Mn_4CaO_5 cluster and functions as an exogenous electron donor during measurement. The pellet obtained by centrifugation was sandwiched between two CaF_2 plates (25 mm diameter). One of the CaF_2 plates has a circular groove (10 mm inner diameter, 1 mm width), and the sample cell was sealed with silicone grease laid on the outer part of the groove (Noguchi and Sugiura 2001). The sample temperature was adjusted to 283 K by circulating cold water in a copper holder.

Light-induced $S_2Q_A^-/S_1Q_A$ and Q_A^-/Q_A FTIR difference spectra were recorded using a Bruker VERTEX 80 spectrophotometer equipped with an MCT detector (InfraRed D313-L). Flash illumination was performed using a Q-switched Nd:YAG laser (Quanta-Ray INDI-40-10; 532 nm; ~7 ns fwhm; ~7 mJ $pulse^{-1}$ cm^{-2}). Single-beam spectra (10-s scans) were recorded before and after a single flash followed by dark relaxation for 5 min. This cycle was repeated 40–80 times and averaged spectra were used to calculate a light-induced difference spectrum. Spectra measured using a couple

of samples were averaged to improve signal-to-noise ratios.

Results and discussion

Light-induced FTIR difference spectra upon the formation of an $S_2Q_A^-$ charge separated state ($S_2Q_A^-/S_1Q_A$ difference) and only Q_A reduction (Q_A^-/Q_A difference) were measured using intact and Mn-depleted PSII membranes of spinach, respectively (Fig. 1a, red and black lines). An FTIR difference spectrum upon the $S_1 \rightarrow S_2$ transition (S_2/S_1 difference) was obtained by subtraction of the Q_A^-/Q_A spectrum from the $S_2Q_A^-/S_1Q_A$ spectrum so as to cancel the strong band at 1,477 cm^{-1} arising from the CO/CC stretching vibration of the Q_A^- semiquinone anion (Berthomieu *et al*. 1990, Ashizawa and Noguchi 2014) (Fig. 1b). This S_2/S_1 spectrum is virtually identical to the spectrum of spinach PSII membranes reported previously (Noguchi *et al*. 1995, Tomita *et al*. 2009). Prominent bands in the 1,700–1,600 cm^{-1} and 1,450–1,350 cm^{-1} have been assigned to the amide I vibrations (CO stretches) of backbone amides and the symmetric COO^- stretching vibrations of carboxylate groups around the Mn_4CaO_5 cluster, respectively (Noguchi and Sugiura 2003, Nakamura and Noguchi 2016). In the 1,600–1,500 cm^{-1} region, bands of the amide II vibrations (NH bends + CN stretches) of backbone amides and those of the asymmetric COO^- vibrations of carboxylate groups overlap (Noguchi *et al*. 1995). The presence of strong amide I and II bands reflects the perturbation of protein conformations around the Mn_4CaO_5 cluster coupled with the $S_1 \rightarrow S_2$ transition.

The S_2/S_1 difference spectrum of PSII membranes, in which Cl^- ions in WOC were replaced with NO_3^- ions, was obtained in an analogous way (Fig. 1d) as a double

difference spectrum between the Q_A^-/Q_A and $S_2Q_A^-/S_1Q_A$ difference spectra (Fig. 1c). Note that at the present stage it is uncertain whether both of the two Cl^- ions (Cl-1 and Cl-2) were replaced with NO_3^- ions or only one of them was replaced with NO_3^- (Hasegawa *et al*. 2004). NO_3^- binding to PSII was confirmed by a $^{14}NO_3^-$-minus-$^{15}NO_3^-$ difference spectrum (Fig. 2b), which was obtained from the S_2/S_1 difference spectra of $^{14}NO_3^-$- (natural abundance NO_3^-) and $^{15}NO_3^-$-substituted PSII samples (Fig. 2a). The spectrum clearly showed bands at 1,416/1,369/1,330/1,278 cm^{-1} assignable to the asymmetric NO_3^- stretching vibrations (Fig. 2b), whose features are very similar to those in the previous FTIR studies of NO_3^--substituted PSII (Hasegawa *et al*. 2002, 2004, Suzuki *et al*. 2013). The corresponding $^{14}NO_3^-$-minus-$^{15}NO_3^-$ spectrum (Fig. 2d) obtained from the S_2/S_1 difference spectra of PsbP-depleted PSII membranes (Fig. 2c) showed a similar intensity signal, indicating that Cl^- was effectively replaced with NO_3^- in both the intact and PsbP-depleted PSII samples. Band positions at 1,401/1,372/1,344/1,286 cm^{-1} in the PsbP-depleted PSII (Fig. 2d) seem rather different from those in the intact PSII (Fig. 2b), suggesting the changes in the interactions of NO_3^- ion(s) by PsbP depletion, although higher-quality spectra may be necessary to definitely determine the band positions.

Although NO_3^- substitution little affected the feature of the symmetric COO^- region at 1,450–1,300 cm^{-1}, the feature of the amide I region (1,700–1,600 cm^{-1}) was significantly altered in NO_3^--substituted PSII (Fig. 1b,d). The intensities of the peaks at 1,678/1,669 cm^{-1} significantly decreased and minor peaks appeared at 1,697/1,686 cm^{-1}. These changes indicate that protein conformations around the Cl^- ion(s) are perturbed by NO_3^- substitution.

An S_2/S_1 difference spectrum of PsbP-depleted PSII membranes (Cl^--bound PSII) in the 1,800–1,200 cm^{-1} region is presented in Fig. 3*A*a together with the spectrum of intact PSII. Spectral changes are clearly shown in their double difference spectrum (Fig. 3*A*b); prominent bands were observed at 1,683, 1,666, 1,657, 1,649, 1,635 and 1,325 cm^{-1} in the amide I region together with some minor bands at 1,560 and 1,539 cm^{-1} in the amide II region, although no appreciable bands were found in the symmetric COO^- region (1,450–1,300 cm^{-1}). This spectral feature is identical to that of a corresponding spectrum in our previous study (Tomita *et al*. 2009), in which the large amide I changes were attributed to the perturbation of the protein conformations of WOC induced by the removal of PsbP. Note that although PsbQ was also removed together with PsbP by high-concentration NaCl treatment, only PsbP is effective to the protein conformation of WOC, because rebinding of PsbP recovered the spectral features (Tomita *et al*. 2009).

Corresponding S_2/S_1 spectra of NO_3^--substituted PSII membranes and a double difference spectrum are shown in Fig. 3*A*c and 3*A*d, respectively. Similarly to Cl^--bound PSII, the spectral feature in the amide I region (1,700–1,600 cm^{-1}) was significantly changed, whereas that in the symmetric COO^- region (1,450–1,300 cm^{-1}) was little changed. The expanded view of the amide I region of the double difference spectra of NO_3^--substituted PSII is shown in Fig. 3*B* (red line) in comparison with that of Cl^--bound PSII (blue line). Upon NO_3^- substitution, the prominent positive peak at 1,666 cm^{-1} almost disappeared, and the negative peak at 1,683 cm^{-1} was replaced with more complex peaks at 1,694/1,686/1,680 cm^{-1}. In addition, the intensities of the positive peaks at 1,649 and 1,625 cm^{-1} slightly increased. These changes indicate that

PsbP-induced protein conformational changes in WOC were affected by NO_3^- substitution for Cl^-. In other words, we detected specific perturbations of the protein conformations around the Cl^- ions by the depletion of PsbP. It is likely that the largely changed amide I bands at 1,683/1,666 cm^{-1} are attributed to the polypeptide chains surrounding the Cl^- ions in WOC.

The next question is how the PsbP binding/depletion affects the protein conformations at the Cl^- binding sites. The recent spinach PSII structure at a 3.2 Å resolution obtained by cryo-electron microscopy showed the interactions of extrinsic proteins with the intrinsic proteins forming WOC (Fig. 4) (Wei *et al*. 2016). Also, the high-resolution (1.9–1.95 Å) X-ray crystallographic structures of cyanobacterial PSII revealed the detailed structure of WOC involving the Cl^- binding sites (Umena *et al*. 2011, Suga *et al*. 2015). Cl-1 is anchored by N181 and E333 of the D1 protein and K317 of the D2 protein, while Cl-2 is anchored by N338 and F339 of the D1 protein and D354 of the CP43 protein (Umena *et al*. 2011, Suga *et al*. 2015). Here, we assume van der Waals interactions that are determined only by a close contact between subunits, because the higher resolution structures of side chains are necessary to argue electrostatic and hydrogen bonding interactions. PsbP interacts with the D1 protein mainly in the two regions (Fig. 4*A*): the region formed by E140, G141 and K166 in PsbP interacting with P340 and L341 in the C-terminus loop region of D1, and the region formed by T16, S32, K33, N52 and F53 in PsbP interacting with Q310–V313 in the loop region and N322 and R323 in the helical region of D1. The first region is very close to the Cl-2 binding site and may directly affect it, while the latter interaction may be effective to the Cl-1 site. The interaction with the D2 protein exists in the region

formed by K38, E39, A55, and T56 in PsbP interacting with I340–E343 in D2 (Fig. 4*B*). This interaction could affect the Cl-1 site though the C-terminal helix of D2. In addition, D139 in PsbP interacts with A351 in D2 (Fig. 4*B*), which interacts with the loop region of D1 near Cl-1 and hence can affect the Cl-1 site. Furthermore, G101 and G102 in PsbP interact with A331 and Q332 in CP43 near Cl-2 (Fig. 4*B*). These interactions of PsbP with D1, D2, and CP43 may contribute to the protein conformational changes around the Cl^- ions upon PsbP removal. It is noteworthy that similar sites in the D1 and D2 proteins (K310–V313, R323, P340, and L341 of the D1 protein and E343 of the D2 protein) interact with the PsbV extrinsic protein in the cyanobacterium *Thermosynechococcus vulcanus* (Suga *et al*. 2015), suggesting a similar effect on the WOC structure between PsbP in higher plants and PsbV in cyanobacteria. In contrast to PsbP, PsbQ interacts with neither the D1 nor the D2 protein, but interacts with the CP43 protein at sites rather far from the Cl^- ions, which is consistent with the previous FTIR observation that PsbQ binding did not affect the FTIR spectrum (Tomita *et al*. 2009).

It has been known that depletion of PsbP enhances the Cl^- requirement in O_2 evolution, and decreases the activity at a low concentration of Cl^- (Miyao *et al*. 1988, Seidler 1996, Ifuku *et al*. 2008). The results of the present study showed that PsbP binding induces the protein conformational changes around the Cl^- ion(s). It is highly likely that such perturbations of protein conformations change the dissociation constant of the Cl^- ions and/or the energy barrier of Cl^- dissociation from the binding sites. We thus conclude that the PsbP extrinsic protein regulates the Cl^- binding and hence the reaction of WOC by perturbing the protein conformations around the Cl^- binding sites.

References

Ashizawa R., Noguchi T.: Effects of hydrogen bonding interactions on the redox potential and molecular vibrations of plastoquinone as studied by density functional theory calculations. – Phys. Chem. Chem. Phys. **16**: 11864-11876, 2014.

Berthomieu C., Nabedryk E., Mäntele W. *et al.*: Characterization by FTIR spectroscopy of the photoreduction of the primary quinone acceptor Q_A in photosystem II. – FEBS Lett. **269**: 363-367, 1990.

Bricker T.M., Roose J.L., Fagerlund R.D. *et al.*: The extrinsic proteins of Photosystem II. – Biochim. Biophys. Acta **1817**: 121-142, 2012.

Bricker T.M., Roose J.L., Zhang P. *et al.*: The PsbP family of proteins. – Photosynth. Res. **116**: 235-250, 2013.

Chu H.-A.: Fourier transform infrared difference spectroscopy for studying the molecular mechanism of photosynthetic water oxidation. – Front. Plant Sci. **4**: 146, 2013.

Debus R.J.: FTIR studies of metal ligands, networks of hydrogen bonds, and water molecules near the active site Mn_4CaO_5 cluster in Photosystem II. – Biochim. Biophys. Acta **1847**: 19-34, 2015.

Enami I., Okumura A., Nagao R. *et al.*: Structures and functions of the extrinsic proteins of photosystem II from different species. – Photosynth. Res. **98**: 349-363, 2008.

Fagerlund R.D., Eaton-Rye J.J.: The lipoproteins of cyanobacterial photosystem II. – J. Photochem. Photobiol. B **104**: 191-203, 2011.

Grundmeier A., Dau H.: Structural models of the manganese complex of photosystem II

and mechanistic implications. – Biochim. Biophys. Acta **1817**: 88-105, 2012.

Hasegawa K,. Kimura Y., Ono T.: Chloride cofactor in the photosynthetic oxygen-evolving complex studied by Fourier transform infrared spectroscopy. – Biochemistry, **41**: 13839-13850, 2002.

Hasegawa K., Kimura Y., Ono T.: Oxidation of the Mn cluster induces structural changes of NO_3^- functionally bound to the Cl^- site in the oxygen-evolving complex of photosystem II. – Biophys. J. **86**: 1042-1050, 2004.

Ido K., Kakiuchi S., Uno C. *et al*.: The conserved His-144 in the PsbP protein is important for the interaction between the PsbP N-terminus and the Cyt b_{559} subunit of photosystem II. – J. Biol. Chem. **287**: 26377-26387, 2012.

Ifuku K., Ishihara S., Shimamoto R. *et al*.: Structure, function, and evolution of the PsbP protein family in higher plants. – Photosynth. Res. **98**: 427-437, 2008.

Ifuku K., Ido K., Sato F.: Molecular functions of PsbP and PsbQ proteins in the photosystem II supercomplex. – J. Photochem. Photobiol. B **104**: 158-164, 2011.

Ifuku K., Noguchi T.: Structural coupling of extrinsic proteins with the oxygen-evolving center in photosystem II. – Front. Plant Sci. **7**: 84, 2016.

Joliot P., Barbieri G., Chabaud R.: Model of the System II photochemical centers. – Photochem. Photobiol. **10**: 309-329, 1969.

Kakiuchi S., Uno C., Ido K. *et al*.: The PsbQ protein stabilizes the functional binding of the PsbP protein to photosystem II in higher plants. – Biochim. Biophys. Acta **1817**: 1346-1351, 2012.

Kok B., Forbush B., McGloin M.: Cooperation of charges in photosynthetic O_2 evolution-I. A linear four step mechanism. – Photochem. Photobiol. **11**: 457-475,

1970.

Messinger J., Noguchi T., Yano J.: Photosynthetic O_2 evolution. – In: Wydrzynski T., Hillier W. (ed.): Molecular Solar Fuels. Pp. 163-207. Chapter 7. Royal Society of Chemistry, Cambridge 2012.

Miyao M., Fujimura Y., Murata N.: Partial degradation of the extrinsic 23-kDa protein of the Photosystem II complex of spinach. – Biochim. Biophys. Acta **936**: 465-474, 1988.

Nagao R., Tomo T., Noguchi T.: Effects of extrinsic proteins on the protein conformation of the oxygen-evolving center in cyanobacterial photosystem II as revealed by Fourier transform infrared spectroscopy. – Biochemistry **54**: 2022-2031, 2015.

Nakamura S., Noguchi T.: Quantum mechanics/molecular mechanics simulation of the ligand vibrations of the water-oxidizing Mn_4CaO_5 cluster in photosystem II, – Proc. Natl. Acad. Sci. U.S.A. **113**: 12727-12732, 2016.

Nishimura T., Nagao R., Noguchi T. *et al.*: The N-terminal sequence of the extrinsic PsbP protein modulates the redox potential of Cyt b_{559} in photosystem II. – Sci. Rep. **6**: 21490, 2016.

Nishimura T., Uno C., Ido K. *et al.*: Identification of the basic amino acid residues on the PsbP protein involved in the electrostatic interaction with photosystem II. – Biochim. Biophys. Acta **1837**: 1447-1453, 2014.

Noguchi T.: Fourier transform infrared difference and time-resolved infrared detection of the electron and proton transfer dynamics in photosynthetic water oxidation. – Biochim. Biophys. Acta **1847**: 35-45, 2015.

Noguchi T., Berthomieu C.: Molecular analysis by vibrational spectroscopy. – In: Wydrzynski T., Satoh K. (ed.): Photosystem II: The Light-Driven Water:Plastoquinone Oxidoreductase. Pp. 367–387. Springer, Dordrecht 2005.

Noguchi T., Ono T., Inoue Y.: Direct detection of a carboxylate bridge between Mn and Ca^{2+} in the photosynthetic oxygen-evolving center by means of Fourier transform infrared spectroscopy. – Biochim. Biophys. Acta **1228**: 189–200, 1995.

Noguchi T., Sugiura M.: Flash-induced Fourier transform infrared detection of the structural changes during the S-state cycle of the oxygen-evolving complex in photosystem II. – Biochemistry **40**: 1497-1502, 2001.

Noguchi T., Sugiura M.: Analysis of flash-induced FTIR difference spectra of the S-state cycle in the photosynthetic water-oxidizing complex by uniform ^{15}N and ^{13}C isotope labeling. – Biochemistry **42**: 6035–6042, 2003.

Ono T., Inoue Y.: Effects of removal and reconstitution of the extrinsic 33, 24 and 16 kDa proteins on flash oxygen yield in photosystem II particles. – Biochim. Biophys. Acta **850**: 380-389, 1986.

Petrouleas V., Crofts A.R.: The quinone iron acceptor complex. – In: Wydrzynski T., Satoh K. (ed.): Photosystem II: The Light-Driven Water:Plastoquinone Oxidoreductase. Pp. 177-206. Springer, Dordrecht 2005.

Roose J.L., Frankel L.K., Mummadisetti M.P. *et al.*: The extrinsic proteins of photosystem II: update. – Planta **243**: 889-908, 2016.

Seidler A.: The extrinsic polypeptides of Photosystem II. – Biochim. Biophys. Acta **1277**: 35-60, 1996.

Shen J.-R.: The structure of photosystem II and the mechanism of water oxidation in

photosynthesis. – Annu. Rev. Plant Biol. **66**: 23-48, 2015.

Sinclair J.: The influence of anions on oxygen evolution by isolated spinach chloroplasts. – Biochim. Biophys. Acta **764**: 247-252, 1984.

Suga M., Akita F., Hirata K. *et al.*: Native structure of photosystem II at 1.95 Å resolution viewed by femtosecond X-ray pulses. – Nature **517**: 99-103, 2015.

Suzuki H., Sugiura M., Noguchi T.: Determination of the miss probabilities of individual S-state transitions during photosynthetic water oxidation by monitoring electron flow in photosystem II using FTIR spectroscopy. – Biochemistry **51**: 6776-6785, 2012.

Suzuki H., Yu J., Kobayashi T. *et al.*: Functional roles of D2-Lys317 and the interacting chloride ion in the water oxidation reaction of photosystem II as revealed by Fourier transform infrared analysis. – Biochemistry **52**: 4748-4757, 2013.

Tomita M., Ifuku K., Sato F. *et al.*: FTIR evidence that the PsbP extrinsic protein induces protein conformational changes around the oxygen-evolving Mn cluster in photosystem II. – Biochemistry **48**: 6318-6325, 2009.

Uno C., Nagao R., Suzuki H. *et al.*: Structural coupling of extrinsic proteins with the oxygen-evolving center in red algal photosystem II as revealed by light-induced FTIR difference spectroscopy. – Biochemistry **52**: 5705-5707, 2013.

Umena Y., Kawakami K., Shen J.-R. *et al.*: Crystal structure of oxygen-evolving photosystem II at a resolution of 1.9 Å. – Nature **473**: 55-60, 2011.

Vinyard D.J., Ananyev G.M., Dismukes G.C.: Photosystem II: The reaction center of oxygenic photosynthesis. – Annu. Rev. Biochem. **82**: 577-606, 2013.

Wei X.P., Su X.D., Cao P. *et al.*: Structure of spinach photosystem II-LHCII

supercomplex at 3.2 Å resolution. – Nature **534**: 69-74, 2016.

Wincencjusz H., Yocum C.F., van Gorkom H.J.: Activating anions that replace Cl^- in the O_2-evolving complex of photosystem II slow the kinetics of the terminal step in water oxidation and destabilize the S_2 and S_3 states. – Biochemistry **38**: 3719-3725, 1999.

Figure Captions

Fig. 1. $S_2Q_A^-/S_1Q_A$ (a, c, red lines), Q_A^-/Q_A (a, c, black lines), and S_2/S_1 (b, d) FTIR difference spectra of intact (Cl^--bound) (a, b) and NO_3^--substituted (c, d) PSII membranes of spinach. S_2/S_1 difference spectra were obtained by subtraction of the Q_A^-/Q_A spectra from the $S_2Q_A^-/S_1Q_A$ spectra.

Fig. 2 Asymmetric NO_3^- stretching region of the S_2/S_1 FTIR difference spectra of $^{14}NO_3^-$- (a, c, black line) and $^{15}NO_3^-$- (a, c, red line) substituted PSII membranes, and $^{14}NO_3^-$-minus-$^{15}NO_3^-$ double difference spectra (b, d). (a, b) Control (PsbP-intact) PSII; (c, d) PsbP-depleted PSII.

Fig. 3. (*A*) S_2/S_1 FTIR difference spectra of PsbP-depleted PSII membranes (a, blue line; c, red lines) in comparison with those of control (PsbP-intact) PSII membranes (a, c, black lines), and control-minus-PsbP-depleted difference spectra (b, d). (a, b) Cl^--bound PSII; (c, d) NO_3^--substituted PSII. (*B*) Expanded view of the amide I region of the control-minus-PsbP-depleted difference spectra of Cl^--bound (blue line) and NO_3^--substituted (red line) PSII membranes.

Fig. 4. Interactions of PsbP with the D1 subunit (*A*) and the D2 and CP43 subunits (*B*). The protein structures were produced from the PDB data (entry code: 3JCU) of spinach PSII obtained by cryo-electron microscopy (Wei *et al*. 2016). Different colors are used to express individual subunits: PsbP (red), D1 (blue), D2 (green), and CP43 (magenta).

The Mn_4CaO_5 cluster, Cl^- ions, and amino acid residues interacting between PsbP and other subunits are shown in balls with van der Waals radii.

Fig. 1

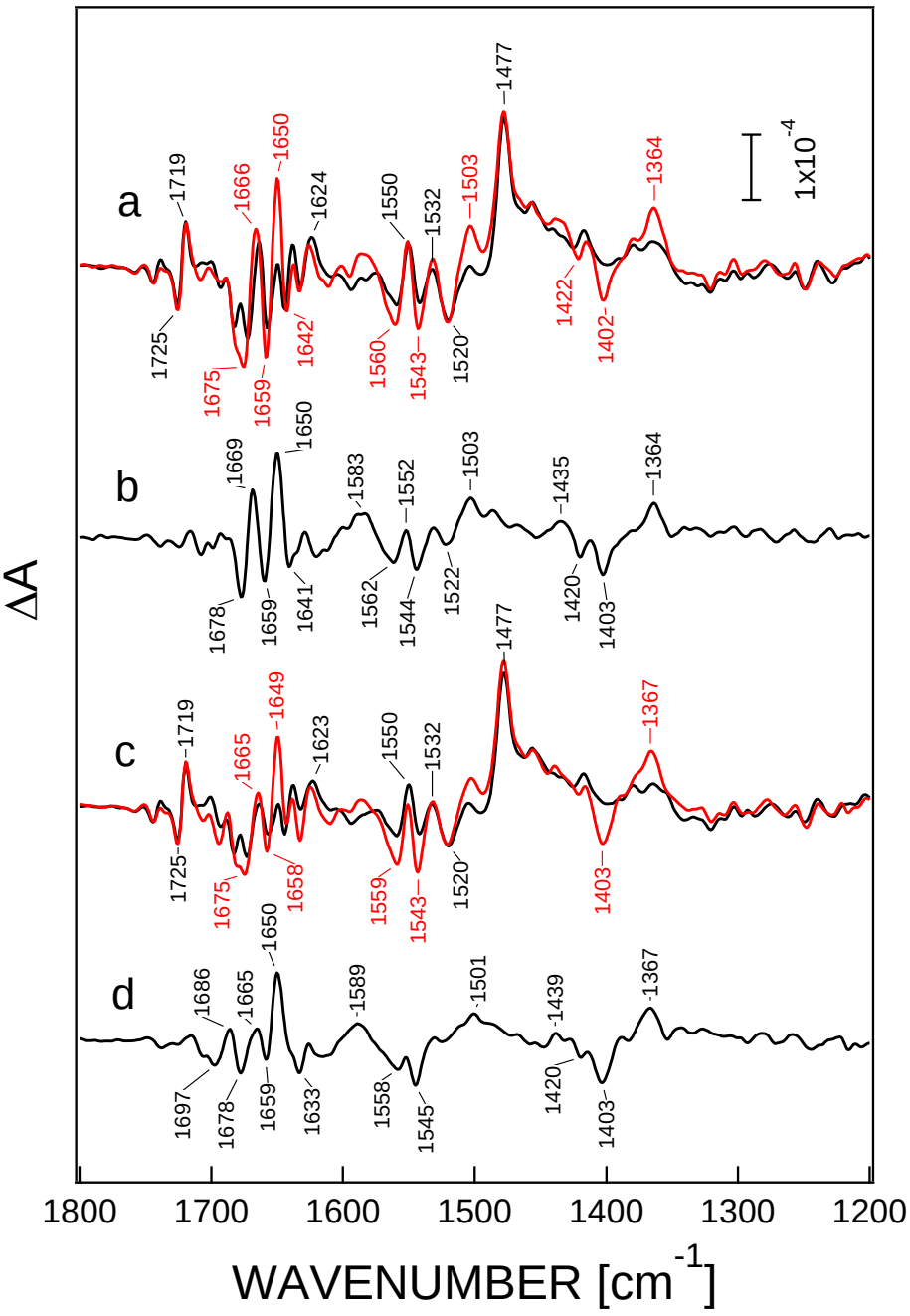
a
1719
1666
1650
1624
1550
1532
1503
1477
1364
1422
1402
1725
1675
1659
1642
1560
1543
1520
1x10-4
b
1669
1650
1583
1552
1503
1435
1364
1678
1659
1641
1562
1544
1522
1420
1403
c
1719
1665
1649
1623
1550
1532
1477
1367
1725
1675
1658
1559
1543
1520
1403
d
1686
1665
1650
1589
1501
1439
1367
1697
1678
1659
1633
1558
1545
1420
1403
ΔA
1800
1700
1600
1500
1400
1300
1200
WAVENUMBER [cm-1]

Fig. 2

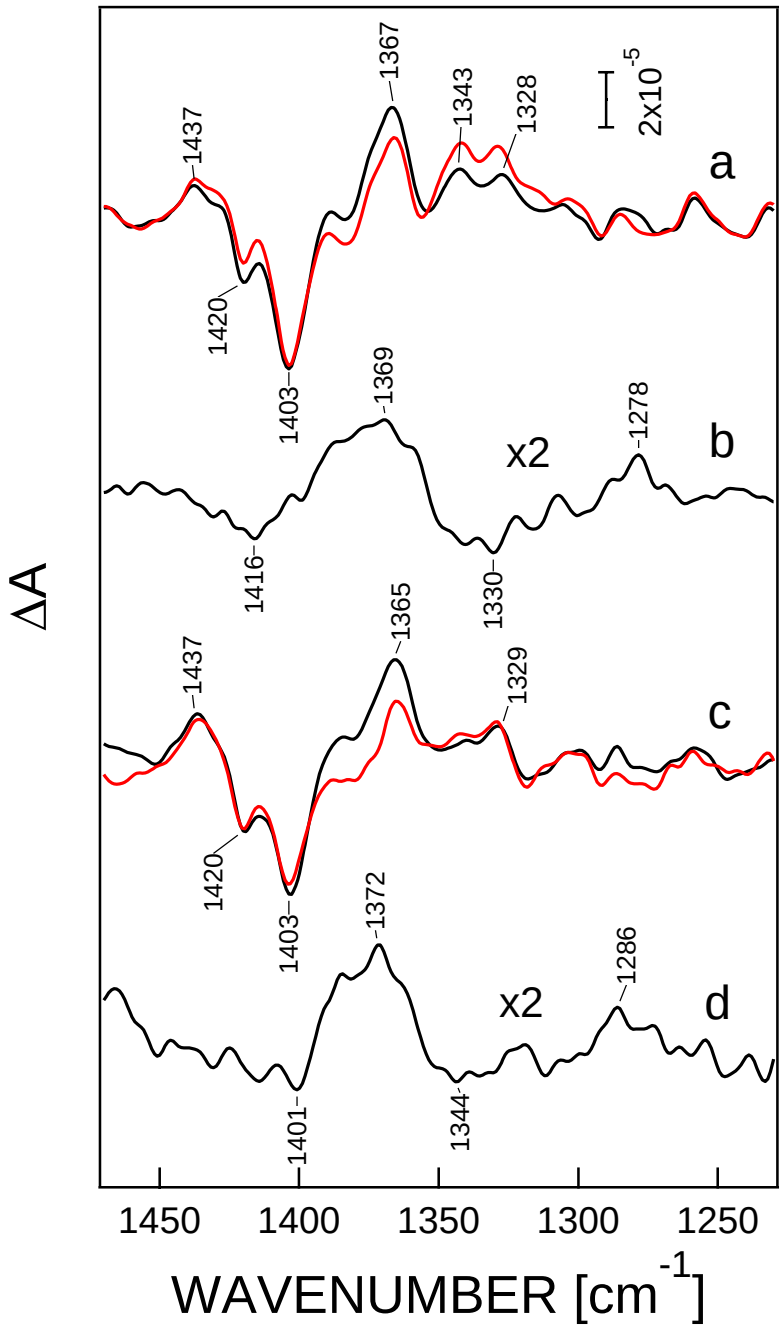
ΔA
1437
1420
1403
1367
1343
1328
2x10-5
a
1369
x2
1278
b
1416
1330
1365
1329
c
1372
1286
d
1401
1344
1450
1400
1350
1300
1250
WAVENUMBER [cm-1]

Fig. 3

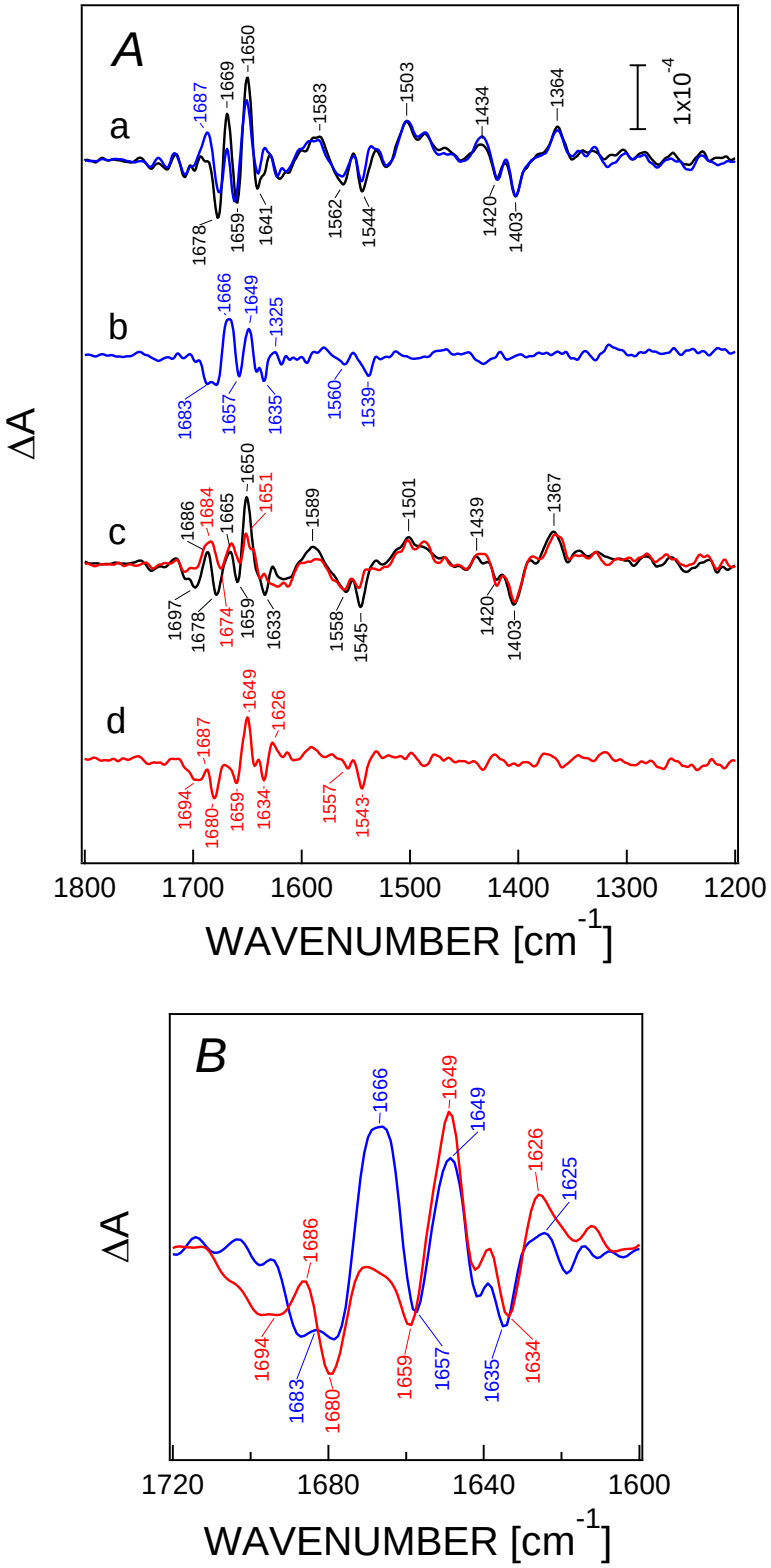
A
a
b
c
d
1687
1669
1650
1583
1503
1434
1364
1678
1659
1641
1562
1544
1420
1403
1x10-4
1666
1649
1325
1683
1657
1635
1560
1539
1650
1686
1684
1665
1651
1589
1501
1439
1367
1697
1678
1674
1659
1633
1558
1545
1420
1403
1649
1687
1626
1694
1680
1659
1634
1557
1543
ΔA
1800
1700
1600
1500
1400
1300
1200
WAVENUMBER [cm-1]
B
1666
1649
1649
1626
1625
1686
1694
1683
1680
1659
1657
1635
1634
ΔA
1720
1680
1640
1600
WAVENUMBER [cm-1]

Fig. 4

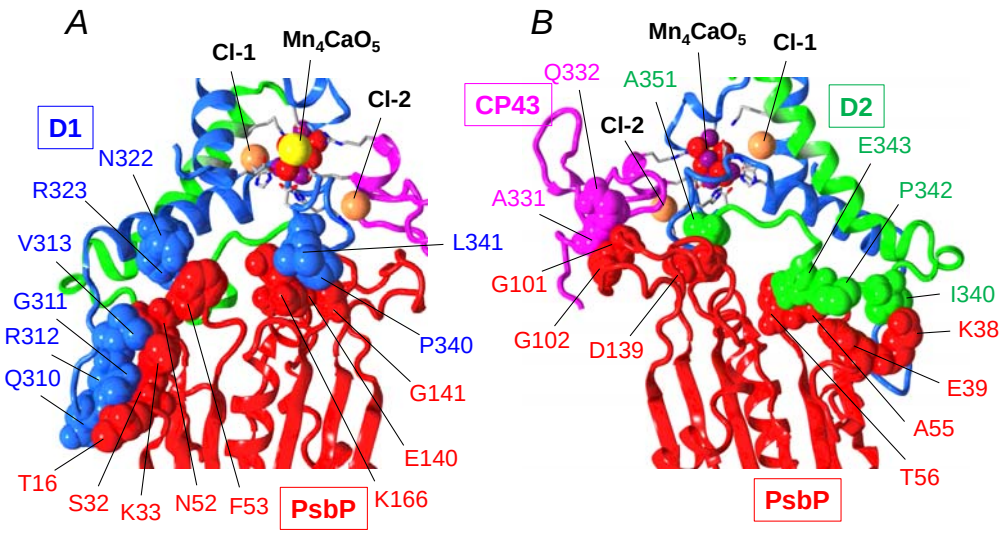
A
Cl-1
Mn4CaO5
Cl-2
D1
N322
R323
V313
L341
G311
R312
P340
Q310
G141
E140
T16
S32
K33
N52
F53
PsbP
K166
B
Mn4CaO5
Cl-1
Q332
A351
CP43
Cl-2
D2
E343
A331
P342
G101
I340
G102
D139
K38
E39
A55
T56
PsbP